A *wingless*-Dependent Polar Coordinate System in *Drosophila* Imaginal Discs

Juan Pablo Couso, Michael Bate, Alfonso Martínez-Arias

The patterning of the imaginal discs in *Drosophila melanogaster* is a progressive process that, like the patterning of the larval epidermis during embryogenesis, requires the activity of segment polarity genes. One segment polarity gene, *wingless*, encodes a homolog of the mouse proto-oncogene *Wnt-1* and plays a prominent role in the patterning of the larval epidermis and the imaginal discs. However, whereas the function of *wingless* in the embryo is initially associated with a pattern of stripes along the anteroposterior axis that are part of a Cartesian coordinate system, it is shown here that during imaginal development *wingless* is associated with a pattern of sectors that provide references for a polar coordinate system homologous to that postulated in a well-known model for the regeneration of insect and vertebrate limbs.

The adult epidermis of *Drosophila melanogaster* develops from specialized groups of cells, the imaginal discs. The cells that form the discs are set aside from the larval epidermis during embryogenesis (*1*, *2*); they proliferate during larval life and differentiate during pupal metamorphosis. Early events in the patterning of the imaginal discs, such as the subdivision into anterior and posterior compartments as a result of the activity of the *engrailed* (*en*) gene, take place during embryogenesis (*3*, *4*). In the embryo, the information necessary for patterning every segment is generated by the products of the segment polarity genes, which encode a group of proteins that mediate and implement cell interactions (*5*, *6*). Spatial cues generated by the segment polarity genes are also required for the formation of the imaginal precursors in the embryo; for example, no imaginal tissues can be recovered from embryos mutant for the segment polarity gene *wingless* (*wg*) (*7*), and the expression of *Distalless* (*Dll*), which correlates with the specification of leg discs, is dependent on proper segment polarity gene expression (*8*). In addition, most segment polarity genes are required during the development of the adult epidermis, suggesting that the segment polarity genes are also involved in pattern formation during imaginal development (*9*–*14*).

A correlation between segment polarity gene expression and function during embryogenesis is slowly emerging (*5*, *6*, *15*). Attempts to establish similar correlations during the development of the adult epidermis have focused on studies of segment polarity gene expression in the third larval instar, when the imaginal discs are large and accessible (*11*–*14*). However, if segment polarity genes show dynamic patterns of expression during imaginal development, as they do during embryogenesis, the requirement for these genes might be related to patterns of expression in discs at stages earlier than the third larval instar. For example, the defects in the adult epidermis associated with the absence of *wg* function are not easy to reconcile with the pattern of expression of the *wg* gene in the third-instar larval discs (*13*, *14*) despite observations that *wg* behaves nonautonomously in clones and encodes a secreted product (*10*, *16*, *17*). We show here that an understanding of the role of the segment polarity genes in the patterning of the adult epidermis requires studying patterns of expression and function of these genes at all stages of imaginal development.

We now describe the expression of *en* and *wg* in the imaginal discs from the time the imaginal disc cells segregate from the larval epidermis until the end of the third larval instar. To assess the significance of these patterns of expression, we have perturbed the function of the *wg* gene at different stages of imaginal development and have analyzed the effects of these perturbations on the pattern of the adult cuticle.

Expression of *en* and *wg* in the primordia of the imaginal discs. When the germ band retracts one-third of the way through embryogenesis, epidermal cells undergo changes in shape that lead to alterations in the organization of the stripes of *en* and *wg* expression (Fig. 1, A and B). During this process, the cells that will give rise to the imaginal discs behave differently from the epidermal cells of the larva (*1*). In each leg disc primordium, the region that expresses *wg* changes from a stripe until it occupies a sector of the circular primordium (Fig. 1C). At about 12 hours of development, the primordial cells invaginate from the epidermis and shortly afterward the discs can be identified in flat preparations as subepidermal clusters of cells (*1*) (Figs. 1D and 2A) with characteristic patterns of *wg* and *en* expression. In each of the leg disc primordia, cells in the anterior half express *wg*; posterior to them, there are about four or five cells that express *en* and several other cells that do not express either *wg* or *en* (Fig. 1D). The wing and haltere discs arise from a region of the epidermis devoid of *wg* expression, and their cells also lack *wg* expression (Fig. 1). However, 10 to 13 cells in each posterior wing primordium and 6 to 7 cells in the posterior haltere primordium express *en* (Fig. 1D).

We have followed the expression of *wg* and *en* in the imaginal discs during larval development by staining either directly for their gene products or for the expression of a *lacZ* gene regulated by the *en* or *wg* promoter so that *lacZ* expression mimics the endogenous patterns of *en* or *wg* expression (*18*, *19*). The discs were identified by their relative positions and morphological features until the third instar. The absence of fate maps for first- and second-instar discs has made it difficult to assess precisely the spatial localization of the patterns of expression. Nonetheless, the anteroposterior (AP) axis was inferred from the expression of *en*, which should remain associated with the posterior region of the discs during development (*4*, *18*, *20*), and the presumptive proximal end of each disc was determined as the point through which the disc is attached to the larval epidermis.

In first-instar larvae, the imaginal discs are arranged with respect to the larval epidermis (*21*–*23*), much as they are in the embryo (*1*). During this period, *wg* is expressed in all of the leg discs in a region comparable to that seen in the embryo, that is, in part of the anterior portion of the disc (Fig. 2A). The wing and haltere discs, which appear as oval structures with a lumen and attachments to the tracheal system and the epidermis, were devoid of *wg* expression at this stage (Fig. 2E).

During the second larval instar, the discs begin to change their shapes and positions relative to the larval epidermis (Fig. 1) to those characteristic of the third instar (*22*). At this time, the expression of *wg* in the leg discs (Fig. 2B) was similar to that of *wg* in the first-instar discs, whereas *en* was expressed in cells located more posteriorly with reference to the AP axis of the animal. At the beginning of the second instar, *wg* expression was detected for the first time in the distal part of both the haltere and the wing discs. As these discs developed, *wg* expression occupied a quadrant of about 30 cells within the distal region of the disc.

The authors are in the Department of Zoology, University of Cambridge, Cambridge CB2 3EJ, United Kingdom.

The position of these cells suggests that they reside in the anterior part of the disc and abut those expressing *en* (Fig. 2F). The cells expressing *en* occupied an adjacent sector which filled almost half of the disc (Fig. 3B). This pattern of *wg* expression was similar to that displayed by the leg discs during early stages (Fig. 1C). Although the lack of a fate map at this stage made it

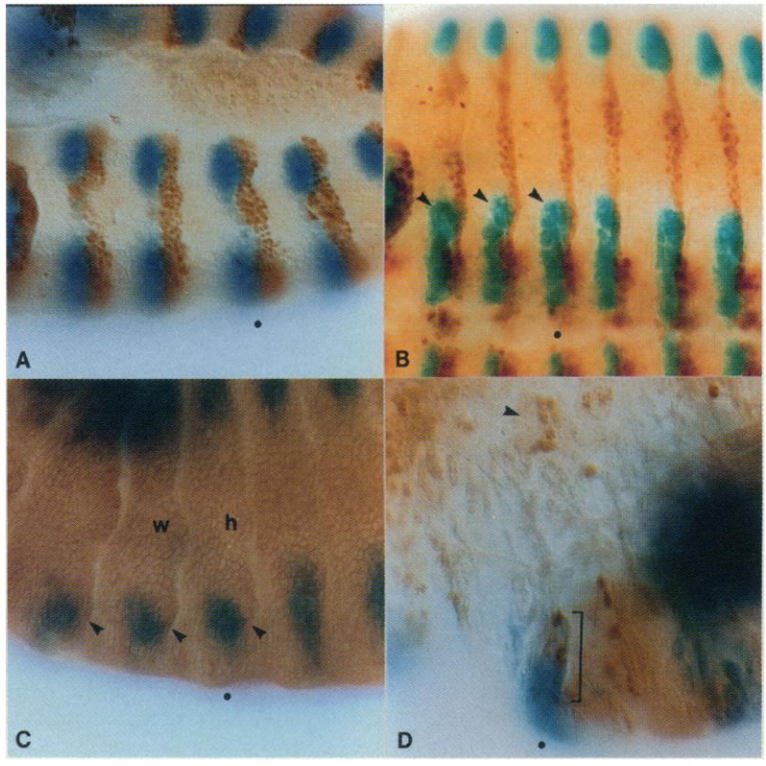

Fig. 1. Patterns of *wg* and *en* expression in the imaginal primordia during embryogenesis. The position of the third thoracic segment is indicated by a dot at the level of the ventral midline (*37*). Anterior is to the left and dorsal is up. (**A**) Epidermis of a wild-type embryo about 7 hours after egg laying (AEL). The blue staining reflects activity staining for β-galactosidase, which is expressed from the *wingless* promoter at the *wg* locus in the same pattern as the endogenous *wg* transcript. The brown nuclei reflect the location of en protein, which was localized with an antibody for en. Both the *wg* and the *en* genes are expressed in stripes, although at this stage each *wg* stripe has split at the level of the tracheal pits. (**B**) Epidermis of an embryo shortly after germ band retraction, about 11 hours AEL, stained as in (A). The initial stripe of *wg* is now clearly split into a ventral stripe and a dorsal patch. It can be seen that, associated with the formation of the leg discs (arrowheads), the stripes of *wg* expression acquire a characteristic shape in the thorax. The leg discs form at the edge of the ventral stripe of *wg* expression (*8*). (**C**) Epidermis of an embryo before the invagination of the disc primordia, stained for β-galactosidase activity, which reflects *wg* expression (blue). The cell outlines are revealed with an antibody against spectrin (*38*). The expression of *wg* is clearly different in the thorax and in the abdomen. The position of the third (last) thoracic segment is indicated by the dot. In the incipient leg discs (arrowheads), *wg* expression is restricted to the anterior-ventral sector of the disc. Also, there is no expression in the primordia of the wing (w) and haltere (h) discs. (**D**) The imaginal discs after invagination, stained as in (A) and (B). The plane of focus identifies the discs in the third thoracic segment. In the leg primordium (bracket), three kinds of cells can be identified, some express *wg*, others *en*, and some express neither. The arrowhead shows the expression of en in the haltere disc and the absence of *wg* expression in this primordium.

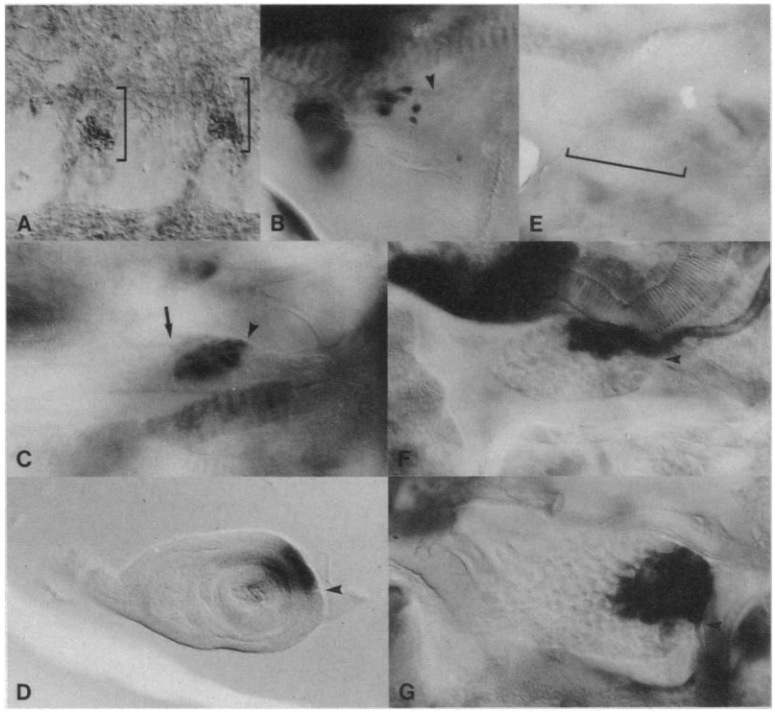

Fig. 2. Patterns of *wg* expression as they relate to the circular and PD organization of the discs. Except for (A) and (D), all the patterns reflect lacZ protein made under the control of the *wg* promoter (*19, 37, 40*). The arrowheads point to the position of the AP boundary. (**A**) Primordia of meso- (second) and meta- (third) thoracic legs in an embryo after dorsal closure (about 13 hours AEL) stained with anti-wg (brackets). Posterior is to the right. The staining is present in the cells of the anterior region of the leg primordia. (**B**) Expression of *wg* in a mesothoracic leg disc of a *wg-lacZ*/+ second-instar larva; posterior is to the right. *en* is expressed in some cells around the attachment to the central nervous system from this stage onward, and this allows us to orient the discs in the AP axis. (**C**) Expression of *wg* in a mesothoracic leg disc of a *wg-lacZ*/+ early third-instar larva (about 72 hours AEL); the upper side of the disc is anterior. The labeled cells occupy a quarter of the disc, with sharp borders in a medial position (arrow) and along the AP boundary, as inferred by comparison with *en* stainings (Fig. 3A). (**D**) Mesothoracic leg disc of a late third-instar larva (about 120 hours AEL) stained with anti-wg; orientation as in (C). The protein can be mapped reliably to the ventral anterior sector of the disc. (**E**) Wing disc (bracket) of a *wg-lacZ*/+ first-instar larva. The larva was stained with anti–β-galactosidase, but no label could be detected in the disc. (**F**) Expression of *wg* in a wing disc of a second-instar *wg-lacZ*/+ larva; posterior to the bottom, proximal and dorsal to the left. Expression is clearly in the distal half of the anterior compartment, as can be noted by the attachment of the trachea (arrowhead, compare with Fig. 3B), which provides a landmark for the boundary between the expression of *wg* and *en* at this stage. Notice the similarity of this pattern of expression with that of the leg disc in (C). (**G**) Expression of *wg* in the wing disc of a late second-instar *wg-lacZ*/+ larva. The signal is present in a sector of the disc and appears to abut a region that lies around the AP boundary. Notice the homology of this expression with that of *wg* in a late leg disc that is shown in (D).

difficult to decide which structures within the anterior region of the disc expressed *wg*, a comparison with the fate map of older discs suggests that the *wg* expression might be associated with either the distal or the ventral-anterior presumptive region (*24*).

In early third-instar larvae, except for a thin stalk, the leg discs appear completely detached from the epidermis. Their morphology, as well as the patterns of *en* and *wg* expression, were similar to those of the wing and haltere discs in the second instar (compare Fig. 2C with 2F and 3A with 3B). Because the overall shape of the leg discs remains constant during the third instar, it would appear that *wg* expression is restricted to the presumptive ventral-anterior sector of the disc (Fig. 2D). This expression pattern is consistent with the finding that this region tends to be deleted in *wg* mutants (see below).

The wing and haltere imaginal discs of early third-instar larvae are similar to those of mature third instar, although they are smaller and lack the conspicuous foldings and grooves of third-instar discs (*22*). The pattern of *en* expression in these discs remained restricted to the posterior region during the third instar and has been described (*25*). In contrast, the expression of *wg* in the wing and haltere discs underwent a transition during the early third instar. Initially *wg* expression spread over the presumptive distal region (Fig. 4A). As development proceeded, it occupied the whole presumptive distal wing region of the disc, where a stripe with high levels of *wg* expression arose parallel to the minor axis of the disc, in the region that would later become the wing margin (Fig. 4B). In wing discs at late third instar, *wg* was only expressed in a few cells along the presumptive wing margin, in a double ring around the distal region of the wing, and in the notal region over the position of the dorsocentral bristle precursors (Fig. 4C).

A requirement for *wg* in the early patterning of imaginal discs. We studied the requirements for the *wg* product during the early development of imaginal discs with the use of a temperature-sensitive heteroallelic combination, wg^{IL114}/wg^{CX3}. Heterozygous wg^{IL114}/wg^{CX3} flies reared at 17°C emerge and show almost no mutant phenotype, except for variable loss of head structures and the dorsocentral bristles. When these flies were reared at 25°C (the restrictive temperature), they gave rise to adults that failed to emerge and had strong *wg* mutant phenotypes (Table 1). Offspring from the cross $wg^{IL114}/CyO \times wg^{CX3}/CyO$ were collected at 17°C and shifted to 25°C at different stages of development. They were maintained at the restrictive temperature (25°C) either continuously (until the end of development) or for only 12 hours after which they were transferred back to 17°C. The results of these temperature shifts (Table 1) are described as the penetrance of *wg* phenotypes per disc (Fig. 5). Whereas every experiment yielded defective disc derivatives, early exposure to 25°C for 12 hours [between 12 and 24 hours after egg laying (AEL)] and late exposure to 25°C (from 72 hours AEL until the end of development) produced aberrations in the dorsoventral (DV) and proximodistal (PD) axes exclusively in legs. Only exposure to 25°C during the second larval instar (48 to

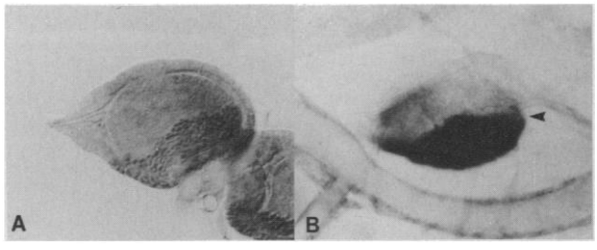

Fig. 3. Expression of *en* during the early stages of imaginal disc development. Discs are orientated as in Fig. 2. (**A**) Third leg disc of an early third-instar larva (about 84 hours AEL) stained with anti-en. The cells expressing en protein occupy a large sector adjacent to the cells that express *wg*. This pattern of expression is similar to that present in wing discs from the second larval instar [compare with (B)]. (**B**) Wing disc of an *en-lacZ*/+ second-instar larva stained with anti–β-galactosidase to reveal *en* expression. The expression of *en* occupies a sector that is bigger and adjacent to that of *wg* expression at the same stage, when the attachment of the trachea (arrowhead) provides a landmark to observe the relative position of the expression of these genes.

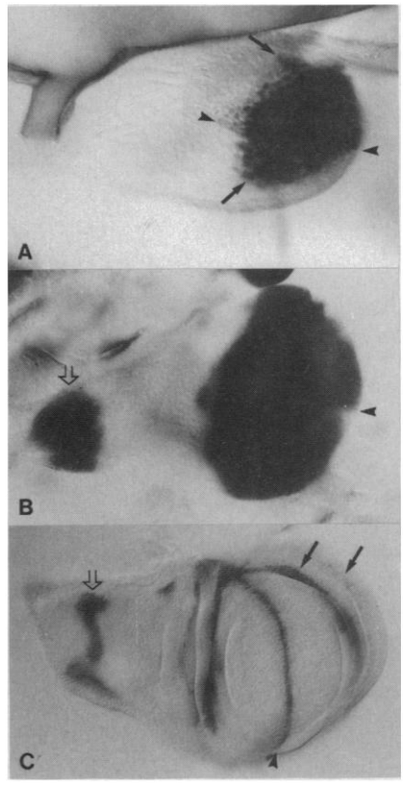

Fig. 4. Pattern of *wg* expression in the wing disc during the third larval instar. Proximal is to the left and distal is to the right. (**A**) Wing disc of an early third-instar *wg-lacZ*/+ larva stained with anti–β-galactosidase. At this stage the pattern of expression is spreading over the posterior compartment (the arrowheads point to the probable position of the AP boundary). The expression in the notum and the stripe along the DV border begin to appear (arrows). (**B**) Wing disc of a mid–third-instar *wg-lacZ*/+ larva after developing the X-gal reaction. The staining occupies the whole distal region and is present on the notum (empty arrow; arrowhead as above). The labeling in the wing seems more intense along the lines of the later pattern [compare with (C)]. (**C**) Wing disc of a late third-instar larva, about 120 hours, AEL stained with anti-wg. The pattern has evolved into two rings around the distal wing (arrows) and a thinner stripe along the wing margin (arrowhead) and across the notum (empty arrow) (*44*).

Table 1. Penetrance of *wingless* mutant phenotypes in wg^{IL114}/wg^{CX3} flies exposed to the restrictive temperature (25°C) during different developmental times. The results are expressed as percentages of affected discs. Data are based on 30 flies or more, except as indicated.

Organ	Affected discs (percent)					
	Continuous		Exposure to 25°C at hours AEL			
	17°C	25°C*	12–24	48–60	72–84	96–end
Legs	5.3	85.5	71.7†	55.5	69.5‡	0.0
Wings	0.0	76.7	0.0	63.3	0.0	0.0
Halteres	4.2	90.0	0.0	95.0	0.1	0.0
Adc bristles	39.2	100.0	36.7	31.3	32.7	88.1

*This set of data (animals continuously raised at 25°C) is based on 15 flies. †Of these legs, 40 percent are missing distal structures and 60 percent have duplications of distal structures. ‡The percentages for these *wg*'s are 20 and 80 percent, respectively. Adc: anterior dorsocentral (*48*).

60 hours AEL) resulted in similar defects in legs, wings, and halteres. These data suggest that the requirement for *wg* in the development of distal structures in the wing and haltere discs is confined to the second instar. This conclusion is supported by the observation that animals exposed to the restrictive temperature for 12 hours at the beginning of the second instar showed a similar percentage of haltere and wing defects as animals continuously raised at the restrictive temperature.

Although exposure to 25°C at any time from embryogenesis to mid-third instar (from 12 to 96 hours AEL) produced abnormal legs, the penetrance of the defects did not reach the maximum observed in flies raised continuously at 25°C. These results suggest that unlike the requirement for *wg* in the wings and the halteres, in the legs there is a continuous requirement for *wg* function from embryogenesis until mid-third instar. In the legs, the abnormalities of DV patterning resulting from exposure to 25°C at 12 to 24 hours AEL were more frequently associated with a loss of distal parts, whereas after a late exposure to 25°C the legs contained perfectly distalized duplications (legend of Table 1). Finally, exposure to 25°C from mid-third instar (about 96 hours AEL) to the end of development resulted in maximal penetrance of the loss of dorsocentral bristles and of abnormalities in the abdomen in flies otherwise indistinguishable from the controls. This late requirement for *wg* can be correlated with the pattern of *wg* expression in the wing discs of late third instar (Fig. 4); wingless is also required at this time for the patterning of the wing margin (*26*).

The polar coordinate model during normal development. Pattern formation in the epidermis of *Drosophila* entails the generation of positional information in a two-dimensional layer of cells and is thought to be the result of the organization of positional information within a Cartesian coordinate system. In such a system, the genes required for the generation of AP information are expressed in parallel stripes that are perpendicular to another set of stripes arranged along the DV axis (*15*). Whereas there is some idea about how this information is translated into a pattern in the embryo (*15*), little is known about how positional information is generated and registered in the imaginal discs in which, in addition to the AP and DV coordinates, there is also a coordinate along the PD axis. In a leg, for example, concentric rings in the corresponding imaginal disc give rise to different pattern elements along the PD axis such as the tarsus or the femur, whereas structures such as compartments, with defined AP and DV coordinates, demarcate stripes along the length of the limb that can be mapped to sectors in the imaginal discs (*24*) (Fig. 6).

Experiments on regeneration of limbs in amphibia and insects led to the suggestion that the patterning of appendages requires a system of circular and PD positional information. These conclusions form the basis of the polar coordinate model (*27, 28*), which provides a set of empirical rules that predict the behavior of limbs and imaginal discs during regeneration. These rules propose that each cell in a field is assigned a positional value and that when two disparate posi-

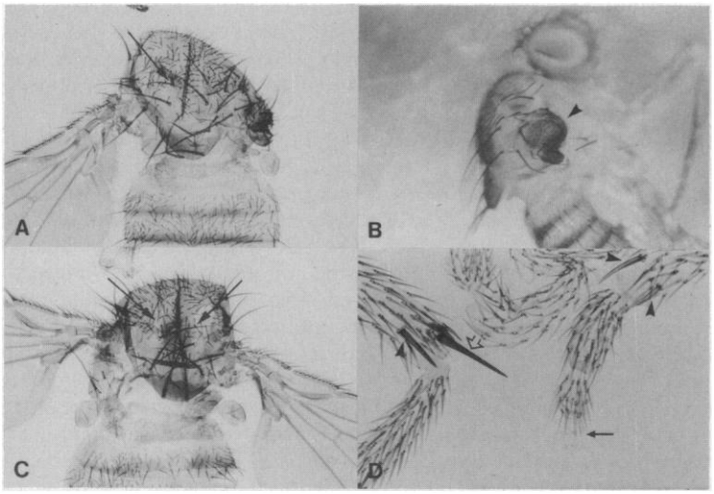

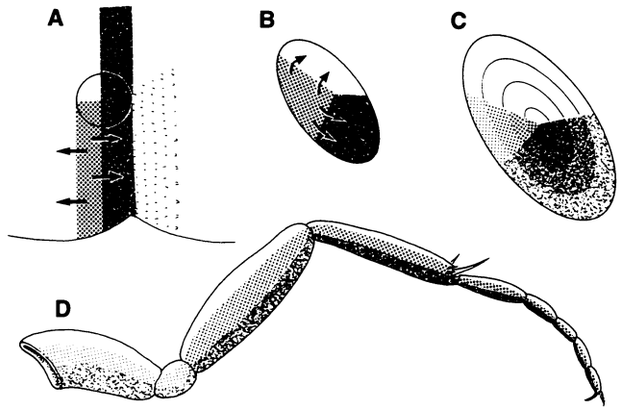

Fig. 5 (left). Mutant *wg* phenotypes in the adult cuticle. (**A**) Thorax of a wg^{1}/wg^{CX3} fly. The heminotum (arrow) on the left is wild-type, whereas the one on the right shows the characteristic *wg* mutant phenotype. The distal derivatives of the wing disc (the wing itself) have been lost and the ventral pleura has been substituted by a mirror-image duplication of the dorsal notum. (**B**) Lateral view of a wg^{1}/wg^{CX3} animal showing the dorso-ventral transformation; the mesothoracic pleura is substituted by a mirror-image duplication of the notum (arrowhead). (**C**) Thorax of a wg^{IL114}/wg^{CX3} animal grown at 17°C, showing the phenotype of loss of dorsocentral bristles (arrows) in an otherwise wild-type notum [compare with the heminotum on the left in (A)]. (**D**) Mesothoracic legs of a wg^{IL114}/wg^{CX3} fly exposed to 25°C for 12 hours between 12 and 24 hours AEL during embryogenesis. The leg on the left has a wild-type phenotype, whereas the leg on the right shows the *wg* transformation. The distal-most elements of the leg have been lost (the fourth and fifth tarsi and the claws; the third tarsus is poorly differentiated, arrow) and the ventral structures are substituted by a mirror image of dorsal ones [the tibial apical bristle (empty arrow) is lost and the preapical one (arrowheads) is duplicated]. This phenotype is analogous to that of the notum shown in (A) and (B) (*45*). **Fig. 6 (right).** Diagrams of the development of positional information during the development of an imaginal disc. Dotted and shaded areas represent regions of *wg* and *en* expression, respectively. (**A**) After germ band retraction, the Cartesian coordinate system that characterizes the larval epidermis results in a parallel arrangement of the expression of *wg* and *en*, which provides information for the generation of the imaginal discs and, eventually, endows them with a basic system of references (*7, 8*). The arrows illustrate different cell interactions significant for patterning. The approximate position of the denticles in the cuticle is indicated and the circumference depicts the approximate position of an imaginal disc. (**B**) In the early disc, the AP and DV coordinates are integrated into an initial set of circular coordinates that demarcate sectors of the disc. We suggest that, as in the larval epidermis (*5, 6, 15, 33*), this initial set of interfaces leads to the generation of new positional values (arrows). Whereas the initial set of larval cell states expands within a sheet of epidermis, the expansion of imaginal states is constrained by the circular geometry of the disc. (**C**) The intercalation of new circular positional values, as suggested in (B), promotes more proliferation near the center of the disc and thus leads to distalization. New PD values are represented as contours within the disc that are likely to be reflected in the expression of genes like *Dll* (*8*) or *esg* (*47*). (**D**) Finally, the imaginal disc unfolds its conical shape during metamorphosis and differentiates the pattern elements of the adult limb. The more distal values arise from the center of the primordium and the more proximal from the periphery.

tional values are apposed (as a result of surgery or injury), the difference in positional values will be smoothed out by the intercalation of intervening values generated by proliferation. During regeneration the limb can reproduce the original complete set of positional values or it can generate mirror-image duplications of an incomplete set in accordance with the shortest intercalation rule (*27*). However, the generation of distal values is always dependent on the generation of circular positional values because (i) local regeneration of circular values can lead to distalization [the distalization rule (*28*)] and (ii) the distalization will be abnormal if a complete set of circular values is not regenerated.

Although the visible *wg* mutant phenotype is not a consequence of cell death and regeneration (*29*), it is reminiscent of the outcomes of regeneration experiments on insect and amphibian limbs. In leg and wing discs, *wg* mutations and the removal of *wg* activity during specific developmental periods cause deletions of ventral structures and are variably associated with mirror-image duplications of dorsal structures and with deletions of distal pattern elements (*14, 29, 30*) (Fig. 5 and Table 1). These defects result in apparently different phenotypes, which probably reflect the sensitivities of individual discs to hypomorphic conditions rather than different functions of the normal gene product. Thus, *wg* appears to participate simultaneously in both the DV and PD organization of the imaginal discs. Although it is possible to find perturbations in DV patterning without perturbations of PD patterning, the converse has not been found. For this reason, we favor the idea that *wg* is required for some aspect of DV organization, which in the imaginal discs is integrated into a set of circular values; this requirement is a prerequisite for the establishment of the PD axis. Thus, the loss of *wg* function causes the failure to specify a complete set of circular values and therefore results in failures of distalization, as was observed for regenerating limbs (*27, 28*).

These observations imply that the rules of the polar coordinate model may apply to the normal development of the limbs and appendages in *Drosophila*. If, as our observations suggest, the development of legs and wings is dependent on a system of circular coordinates, we would expect that the genes responsible for the circular positional values would be expressed in sectors within each disc (Fig. 6). At the times that our temperature shift experiments indicate a requirement for *wg* for distalization, *wg* is expressed in a sector in the wing, haltere, and leg discs. We suggest that this sector represents a wedge of expression that is used to generate circular positional values in the disc (Fig. 6).

This suggestion is further supported by an analysis of our results with reference to the polar coordinate model and the experiments that led to its formulation. The model predicts that, in regenerating limbs with insufficient circular positional values, distal structures will not be produced (*27, 28*). We find that removal of *wg* function from the leg discs early in development, when we postulate that there are few circular values, leads frequently to deficiencies in distal structures. However, removal of *wg* function later in development, when presumably more circular values are present, leads preferentially to duplications of distal structures (legend to Table 1), a result also predicted by the polar coordinate model (*28*).

Our suggestion about the principles that pattern imaginal discs differ significantly from a previous one in which intersections of AP and DV coordinates during imaginal development yield a series of circumferential values that provide the information necessary to generate PD values by intercalation (*31, 32*). From patterns of gene expression in discs of third-instar larvae, it was suggested that the expression of *wg* provides the DV coordinate and the expression of *decapentaplegic* (*dpp*) along the AP compartment boundary provides the AP one (*32*). Whereas our results indicate that *wg* is involved in the process of distalization, they show that at the time it is required for this process, *wg* is expressed in an anterior-ventral wedgelike pattern and that it probably acts through the provision of circular positional values rather than through a contribution to a Cartesian coordinate system. A study of the pattern of expression and requirement for *dpp* in young discs should elucidate its precise function in this process.

The causal relation between circular patterning and distalization during regeneration is explained in the polar coordinate model. In the model, spatial constraints generated during wound healing (*28*) force cells with new circular values into a different configuration that can initiate a new PD coordinate. We observe sectorial patterns of gene expression during normal development that are required for the formation of distal structures. If these expression patterns are related to the generation of circular values, these sets of values will be necessarily smaller or more compressed toward the center of the disc, where circular perimeters are shorter than they are near the periphery. Thus, more circular intercalation of positional values will occur near the center of the disc, and hence the central region might grow faster than the periphery. The geometrical properties of a circular field dictate that this kind of growth will form a cone or a series of concentric folds. We propose that sectorial patterns of gene expression, which are primarily required for circular patterning, could also trigger distalization through this mechanism (Fig. 6). This would explain the consistent relations between the two patterning processes in different experiments and in different organisms such as insects, amphibians, and birds (*28*).

The function of *wg* during imaginal development. The generation of circular values mediated by *wg* during imaginal development is reminiscent of its function during embryogenesis when it is essential for the establishment of positional values in the AP axis. In this process, it is not *wg* alone but its interaction with the neighboring *en*-expressing cells that generates positional values, as a result of the secreted nature of the wg protein (*5, 6, 15, 33*). Perhaps the same mechanism operates during imaginal development. In this case, the expression pattern of *en* within discs should not be considered a stripe but instead a sector that would contain and generate values in the manner predicted by the polar coordinate model. It is relevant in this context that the ability of proximal fragments of wing imaginal discs to regenerate distal structures depends strictly on the presence of both the sector in which *wg* is expressed in the second instar and the AP compartment border, that is, the interface in which the *en* and *wg* sectors are apposed (*34*).

The *wg* function related to circular patterning and distalization appears to have different temporal regulation in the wing and haltere discs when compared with the leg discs. Whereas *wg* function for distalization in the wing and the haltere is restricted to the second larval instar, in the leg discs *wg* is required continuously. Although at present there is no explanation for this, it appears to correlate with the fact that, in the embryos of most arthropods, the development of leg primordia is initiated very early and complete legs are already present at hatching. In contrast, during the development of hemimetabolous insects, the wings arise from a small stump on the dorsal thorax during the last larval molts. It is likely that in the evolution of holometabolous insects, this relative timing has been conserved. Thus, the wings emerge from what is probably notal tissue during the second larval instar in a delayed process of distalization, which is otherwise homologous to the emergence of the legs from the larval epidermis in the embryo.

Embryos develop initially as two-dimensional sheets of cells, and limbs arise from this sheet through a third coordinate, the PD. We suggest that, as a general rule, the generation of this coordinate requires the integration of the AP and DV axes into a set of circular values and that, in *Drosophila*, this step is dependent on the activity of *wg*. Furthermore, our results show that, in

Drosophila, the genes that establish these circular values are expressed in sectors of limb primordia and thus provide a molecular basis for the polar coordinate model. It is possible that our observations can be extended to the development of limbs in other organisms. For example, the early pattern of expression of the *Wnt-5* gene during mouse limb development (*35*) is consistent with the wedge shape that we describe here for *wg* in the developing imaginal discs of *Drosophila*. Furthermore, *En-1* and other homeobox-containing genes are expressed in developing limb buds (*36*). The early patterns of expression of the homeobox-containing genes are also reminiscent of the sectors described above for *wg* and *en*. Whether these patterns of gene expression can also be related to the rules postulated in the polar coordinate model and, in this manner, to their function during the patterning of the limbs remains to be seen.

REFERENCES AND NOTES

1. M. Bate and A. Martínez-Arias, *Development* **112**, 755 (1991).
2. B. Cohen *et al.*, *Mech. Dev.* **33**, 229 (1991).
3. A. García-Bellido, and P. Santamaría, *Genetics* **72**, 87 (1972).
4. G. Morata and P. A. Lawrence, *Dev. Biol.* **56**, 40 (1977).
5. A. Martínez-Arias, *Trends Genet.* **5**, 262 (1989).
6. P. W. Ingham, *Curr. Opin. Genet. Dev.* **1**, 261 (1991).
7. A. A. Simcox *et al.*, *Development* **107**, 715 (1989).
8. S. M. Cohen, *Nature* **343**, 173 (1990).
9. P. A. Lawrence and G. Morata, *Dev. Biol.* **50**, 321 (1976).
10. N. E. Baker, *ibid.* **125**, 96 (1988).
11. J. Mohler, *Genetics* **120**, 1061 (1988); R. G. Phillips, I. J. H. Roberts, P. W. Ingham, J. R. S. Whittle, *Development* **110**, 105 (1990).
12. R. Whittle, *Semin. Cell Biol.* **1**, 241 (1990); A. Wilkins and D. Gubb, *Dev. Biol.* **145**, 1 (1991).
13. M. Peifer *et al.*, *Development* **111**, 1029 (1991).
14. N. E. Baker, *ibid.* **102**, 489 (1988).
15. P. W. Ingham and A. Martinez-Arias, *Cell* **68**, 221 (1992); A. Martinez-Arias in *The Development of Drosophila*, M. Bate and A. Martinez-Arias, Eds. (Cold Spring Harbor Laboratory, Cold Spring Harbor, NY, in press).
16. M. van den Heuvel, R. Nusse, P. Johnston, P. A. Lawrence, *Cell* **59**, 739 (1989).
17. F. González *et al.*, *Mech. Dev.* **35**, 43 (1991).
18. C. Hama, Z. Ali, T. B. Kornberg, *Genes Dev.* **4**, 1079 (1990).
19. J. A. Kassis *et al.*, *Proc. Natl. Acad. Sci. U.S.A.*, in press.
20. T. Kornberg, *ibid.* **78**, 1095 (1981).
21. C. Auerbach, *Trans. R. Soc. Edinb.* **58**, 787 (1936).
22. D. Bodenstein, in *Biology of Drosophila*, M. Demerec, Ed. (Wiley, New York, 1953), pp. 275–361.
23. M. Madhavan and H. Scheneiderman, *Roux's Arch. Dev. Biol.* **183**, 269 (1977).
24. J. Sang, *Genetics and Development* (Longman, London, 1984), p. 295.
25. D. Brower, *EMBO J.* **5**, 2649 (1986).
26. J. P. Couso and A. Martinez-Arias, in preparation.
27. V. French, P. J. Bryant, S. V. Bryant, *Science* **193**, 969 (1976).
28. S. V. Bryant, V. French, P. J. Bryant, *ibid.* **212**, 993 (1981); S. V. Bryant and K. Muneoka, *Trends Genet.* **2**, 153 (1986).
29. G. Morata and P. A. Lawrence, *Dev. Biol.* **56**, 227 (1977); A. A. James and P. Bryant, *ibid.* **85**, 39 (1981).
30. R. P. Sharma and V. L. Chopra, *ibid.* **48**, 461 (1976).
31. H. Meinhardt, in *Developmental Order: Its Origin and Regulation*, S. Subtelny and P. B. Green, Eds. (Liss, New York, 1982), pp. 439–461.
32. W. Gelbart, *Development* **107 suppl.**, 65 (1989).
33. A. Bejsovec and A. Martínez-Arias, *ibid.* **113**, 471 (1991).
34. J. Karlson, *J. Embryol. Exp. Morphol.* **59**, 315 (1980).
35. J. Gavin *et al.*, *Genes Dev.* **4**, 2319 (1990).
36. C. Davis and A. Joyner, *ibid.* **2**, 1736 (1988); P. Dollé, J.-C. Izpisúa-Belmonte, H. Falkenstein, A. Renucci, D. Duboule, *Nature* **342**, 767 (1989); J.-C. Izpisúa-Belmonte, C. Tickle, P. Dollé, L. Wolpert, D. Duboule, *ibid.* **350**, 585 (1991).
37. In these experiments, we have used a line that expresses the *Escherichia coli* β-*galactosidase (lacZ)* gene under the control of *wingless:sli/CyO, enlacZ11::wg* (*19*); in other figures we refer to wild-type animals from this line as *wg-lacZ*/+. The expression of this construct during embryogenesis and throughout the third-instar larval stage was identical to that of the endogenous *wingless* gene as assessed in double-label experiments (J. P. Couso and A. Martinez-Arias, unpublished data). Double-label experiments for antibody and β-galactosidase activity were performed as standard antibody staining (*39*) except that 80 percent ethanol was used instead of methanol to remove the vitelline membrane of the embryos.
38. J. Pesacreta *et al.*, *J. Cell Biol.* **108**, 1697 (1989).
39. M. Ashburner, *Drosophila: A Laboratory Manual* (Cold Spring Harbor Laboratory, Cold Spring Harbor, NY, 1989), pp. 165–167.
40. In some instances (early to late third-instar larvae), we have stained discs for wg protein and observed a similar pattern of expression to the one reported here (J. P. Couso, unpublished data). Flat dissection of embryos were done according to (*41*), and those of larvae as described in (*42*). Staining protocols were carried out as described in (*17*) except in (Fig. 2D), where the disc was dissected out and stained as in (*43*). The antibodies to wg used in our study have been described (*16, 17*).
41. M. Bate, *Development* **110**, 791 (1989).
42. ——— *et al.*, *ibid.* **113**, 79 (1991).
43. R. A. White and M. Wilcox, *Cell* **39**, 163 (1984).
44. Generals procedures were followed as described in (*37, 40*). In (B), the X-gal reaction (*39*) was performed on flat dissected larvae (*42*) instead of the antibody staining. (C) As stated for Fig. 2D in (*40*).
45. The adult flies were dissected, heated in 10 percent KOH, dehydrated, and mounted in phenol. The experimental conditions as well as genetic information concerning the wg^{CX3} and wg^{IL114} alleles are discussed below (*48*). wg^{1} is the original adult viable allele of *wg*; it is probably associated with a regulatory mutation (*30, 46*).
46. N. E. Baker, *EMBO J.* **6**, 1765 (1987).
47. M. Whiteley *et al.*, *Mech. Dev.* **36**, 117 (1992).
48. Eggs were collected for a 4-hour period at 17°C on agar plates and transferred to standard medium after hatching. Animals were maintained at 17°C and exposed to 25°C during the periods shown in Table 1. Developmental ages are described in hours after egg laying (AEL) at 25°C; at this temperature embryogenesis spans from 0 to 24 hours AEL, the second instar occurs between 48 and 72 hours AEL, and the third instar is between 72 and 120 hours AEL. Phenotypes were scored under dissecting and compound microscopes. The wg^{IL114} protein is not secreted at 25°C (*17*), but is largely functional at 16.5°C (*10, 26, 33*). The pupal-lethal allele wg^{CX3} contains a regulatory mutation (*14, 46*), which affects the expression and function of *wg* in the imaginal discs but not in the epidermis of the embryo (J. P. Couso and A. Martínez-Arias, unpublished data). Thus, the genetic constitution wg^{IL114}/wg^{CX3} provides a temperature-sensitive mutant condition with a phenotype restricted to imaginal function. Experiments in which homozygous wg^{IL} adults are obtained give the same results as those described here, except for a poor viability that has precluded us from obtaining a significant number of individuals.
49. *Note added in proof.* Patterns of gene expression similar to those described here have been reported by J. Williams, S. Paddock, S. Carroll, *Development*, in press. These patterns are consistent with our functional interpretation of sectors of gene expression.

50. J.P.C. carried out some of this work supported by a short-term EMBO fellowship and an F.P.U. fellowship from the Spanish Ministerio de Educación y Ciencia. The research of M.B. and A.M.-A. is funded by The Wellcome Trust. We thank A. García-Bellido for discussions throughout the work; M. Baylies and R. Drysdale for comments on the manuscript; N. Perrimon for flies; M. van den Heuve and R. Nusse for antibodies; and R. Phillips and R. Whittle for communicating and discussing results prior to publication.

14 September 1992; 30 December 1992